

A BANDPASS $\Sigma\Delta$ A/D CONVERTOR FOR A DIGITAL AM RECEIVER

Stephen Jantzi, Richard Schreier, Martin Snelgrove

University of Toronto, Canada

ABSTRACT

This paper illustrates the design methodology for analogue-to-digital convertors based on bandpass sigma-delta *modulation*. A digital AM receiver is used as the application to guide the design process.

1. INTRODUCTION

Sigma-delta analogue-to-digital convertors are widely used for high resolution A/D conversion. The benefits of these oversampled noise-shaping convertors include inherent linearity, reduced anti-aliasing filter complexity, high tolerance to circuit imperfection and a system architecture that lends itself well to switched-capacitor implementation: see Candy and Temes (1), Norsworthy et al (2) and Boser and Wooley (3).

Traditional $\Sigma\Delta$ convertors place noise transfer-function zeros near $\omega_0=0$ in order to null quantization noise in a narrow band around DC. This noise-shaping concept was extended in Schreier and Snelgrove (4) to the bandpass case, wherein the noise transfer-function zeros are placed at a non-zero frequency, ω_0 . Quantisation noise is nulled in a narrow band around ω_0 so that the output bit-stream accurately represents the input signal in this narrow band.

For narrow-band signals away from DC, the band-reject noise-shaping of a bandpass $\Sigma\Delta$ convertor results in high signal-to-noise ratios at significantly lower sampling rates than required for lowpass $\Sigma\Delta$ convertors. An amplitude-modulated (AM) radio frequency signal is eminently suited to this scheme, so an AM receiver has been chosen to illustrate the design process. The advantages of using bandpass $\Sigma\Delta$ in this application are many: the mixer stage and IF amplifiers become unnecessary, resulting in a vastly reduced component count; the use of digital signal processing makes possible excellent selectivity and provides the means to cope with multiple standards in stereo AM; and placing the analogue/digital interface closer to the antenna results in a more robust system with improved testability.

The application is a side issue, as this paper is really about the design of bandpass $\Sigma\Delta$ convertors. Nonetheless, we need some specifications to guide the design process. The commercial AM broadcast band is 540kHz to 1600kHz, with stations occupying a 10 kHz wide band. Available AM receivers offer signal-to-noise ratios of about 50 dB over a 60 dB dynamic range. Our system should be designed for comparable performance

Figure 1 illustrates the essential features of an AM receiver built around a bandpass $\Sigma\Delta$ modulator. The radio-frequency (RF) amplifier amplifies the signal of interest and provides the required anti-aliasing. The bandpass $\Sigma\Delta$ modulator converts the analogue signal to a high-speed bit-stream which is subsequently filtered and subsampled by a narrow-band bandpass filter/decimator. The multi-bit output of the decimator is passed to a digital signal processor

(DSP) for further filtering and decimation. The DSP must also implement the appropriate demodulation algorithm.

The paper is divided into sections that reflect the various stages in the design process. Section 2 discusses the design of signal and noise transfer functions for bandpass $\Sigma\Delta$, and chooses the particular modulator needed to fulfill our design goals. Section 3 discusses circuit topology, and a structure is chosen that is insensitive to circuit non-idealities. Section 4 examines some circuit-design considerations, and presents simulation results. Finally, Section 5 discusses the decimation and demodulation requirements of the system.

2. TRANSFER-FUNCTION DESIGN

2.1 Band Location

The ratio of the sampling frequency to the centre frequency of the modulator is the first design decision. Making this ratio large increases the oversampling ratio (defined as one-half the sampling rate divided by the width of the band of interest) and hence improves the performance achievable by a modulator of a given order, but can lead to unrealistically high clock rates. Making this ratio small puts increased demands on the anti-aliasing filter. An additional *consideration is that ratios that are integers or fractions with a small denominator allow for innovation in both circuit design and decimation.*

For the design at hand, a ratio of four is a good compromise, so that the normalised center frequency is at $\pi/2$. The sampling rate must then be tunable over the range 2.16 MHz to 6.40 MHz which is reasonable for switched-capacitor filters. This gives us an oversampling ratio which increases from 108 at the low end of the AM band (1.08 MHz/10 kHz) to 320 at the high end of the band.

Since the normalised center frequency is $\pi/2$, the **first** image that gets aliased in-band is located at three times the current centre frequency. When tuned to 540 kHz the first image is at 1620 kHz which, by its proximity to the AM band, precludes the use of a fixed anti-aliasing filter. Thus the RF stage must be tuned in tandem with the bandpass modulator in order to provide the required anti-aliasing. In addition, as the modulator is tuned across the AM band the relative bandwidth of the signal decreases from 2% to 0.6%, necessitating that the DSP implement a variable-bandwidth filter

2.2 Some Noise Transfer Functions

Replacing the quantiser with an additive noise source produces the linear model of a $\Sigma\Delta$ modulator. In this model, the transfer function from the noise source to the modulator output is called the noise transfer function (NTF) and is the key parameter in a $\Sigma\Delta$ modulator.

Table 1 lists the signal-to-noise ratios (SNR) of several bandpass modulators operated at the low end of the AM band. The NTFs of these modulators were second, fourth or sixth order, with zeros placed either coincidentally at $\pi/2$ or optimally spread across the band

of interest to maximise the SNR, and were chosen to have a maximum gain of less than 1.6 (4 dB). The maximum gain constraint is a rule-of-thumb due to Lee (5) that tries to ensure the stability of the resultant $\Sigma\Delta$ modulator, and for these four NTFs it appeared to succeed.

Low-order transfer functions are preferable because they yield simple modulators. Coincident zeros simplify the design process and may allow innovative circuits to be used. However, with standard switched-capacitor circuits, one can easily use optimised zeros and gain an SNR advantage over circuits which implement coincident zeros.

TABLE 1 – Simulated performance, at the low end of the AM band, of bandpass modulators with different noise transfer functions.

Transfer Function		SNR (dB) (half-scale input)
Order	Zeros	
2	—	55
4	1, coincident	78
4	optimised	83
6	coincident	98
6	optimised	108

In our system, the RF amplifier is assumed to contain automatic gain control (AGC), so that the dynamic range required by the bandpass modulator is considerably less than the 60 dB specification. However, if a strong station swamps the desired one, the AGC cannot raise the power of the desired signal to 0 dB. To allow for this possibility, our circuit must possess an adequate SNR for a range of signal levels. The fourth-order modulator with optimised zeros gives greater than 50 dB SNR for inputs over a 30 dB range, and this is deemed to be an adequate allowance for signal skew.

The chosen NTF is displayed in Figure 2a as a pole-zero plot, and in Figure 2b as a magnitude response. The response is band-reject, has an approximately equiripple stopband with 61.7 dB average attenuation across the band of interest, and has an out-of-band gain of 1.58.

2.3 The Signal Function

In the linear model, the signal transfer function (STF) is the transfer function from the modulator input to the modulator output. If the STF is chosen to have the same poles as the NTF, some filtering can be done on the input at almost no cost. The zeros of the STF are chosen so that the in-band gain is flat and the out-of-band gain is small. Constant in-band gain preserves the signal of interest while small out-of-band gain improves the stability of the modulator by effectively reducing the amplitude of out-of-band signals.

Figure 2a plots the poles and zeros of the STF, and Figure 2b plots its magnitude response. The STF has four poles but only three zeros due to our choice of the cascade-of-resonators structure discussed in Section 3.2. The STF is bandpass, has a wide, flat (within 0.006 dB) passband extending well beyond the band of interest, and has moderate out-of-band attenuation. The 0.5 dB out-of-band gain peaks are an undesirable consequence of having only three zeros in the STF.

3. CIRCUIT TOPOLOGY

3.1 Block Diagram

In a switched-capacitor circuit, capacitor ratios set the coefficients of a structure. Mismatch in these ratios alters the NTF, which lowers the amount of in-band noise attenuation and thus lowers the SNR. A structure whose NTF zeros are insensitive to capacitor mismatch will not suffer severe SNR degradation when fabricated.

The general block structure shown in Figure 3 is able to realise many of the present structures used for $\Sigma\Delta$. Replacing the quantiser by an additive noise source allows one to find H , the NTF:

$$H(z) = \frac{1 - AB}{1 - AB - AC} \quad (1)$$

One choice is $B = -I$, $C = I$, and $A = H - I$. This results in a simple structure which yields many insights into the operation of a $\Sigma\Delta$ modulator. However, it has *poor* sensitivity *properties* as the zeros of H depend on both the zeros and poles of A .

One would like the zeros of H to depend on a single term in order to minimise their dependence on circuit coefficients. The numerator of H can be made dependent on one term by setting either A or B to zero. Setting A to zero removes the modulator feedback term and makes $H = I$, a useless result.

Setting B to zero and C to one makes the poles of A responsible for the zeros of H . A must realise the transfer function $I - 1/H$ in order to give an NTF of H . The STF is DH , and by designing it to have the same poles as H , the D block can share the hardware used in A .

3.2 Block Realisation

A block realisation should be chosen such that the poles of $1 - 1/H$ are insensitive to capacitor mismatch. Using the linear model, and assuming a noise spectral density of $1/3$, an analytical calculation of the in-band noise power, N_0^2 , is possible:

$$N_0^2 = \frac{1}{3\pi} \int_{\omega_1}^{\omega_2} H(e^{j\omega}) H(e^{-j\omega}) d\omega \quad (2)$$

The goal in bandpass $\Sigma\Delta$ is to have a small value of N_0^2 , and for our modulator this figure-of-merit is -86.8 dB.

The cascade-of-integrators structure shown in Figure 4 was used for a spread-zero low-pass $\Sigma\Delta$ system by Lee (5). The coefficients B_{1-4} set the zeros of the NTF, and the coefficients A_{1-4} set its poles. To simulate the effects of manufacturing tolerances on modulator performance, all capacitor ratios were randomly varied by up to 0.5%, and N_0^2 calculated. With this tolerance, fewer than 1% of the perturbed modulators had $N_0^2 < -60$ dB. This SNR degradation makes the cascade-of-integrators structure unsuitable for our narrow-band bandpass $\Sigma\Delta$ modulator.

The **cascade-of-resonators** structure shown in Figure 5 was used for a spread-zero low-pass $\Sigma\Delta$ system by Ferguson et al (6). The R coefficients set the zero locations of the NTF, and the B and R coefficients set its poles. With the same 0.5% capacitor ratio tolerance, which is readily obtainable in current switched-capacitor technology, 95% of the modulators had $N_0^2 < -83$ dB. As for the stability constraint, all the modulators tested had maximum NTF gains below 1.61. These two facts indicate that the cascade-of-resonators structure has adequate sensitivity properties for our application.

A summary of the sensitivity analyses for the two structures can be seen in the histograms of Figure 6. Each test examined a set of 50k perturbed modulators. It is clear that the cascade-of-integrators structure is markedly inferior to the cascade-of-resonators structure.

Parallel form and the N-path technique have been considered as possible alternative structures. However, parallel form is not suitable as it represents a partial-fraction expansion of a rational function, and thus cannot easily form the coincident or nearly-coincident poles of H^{-1} . Gregorian and Temes (7) have shown that N-path realisations have excellent sensitivity properties for narrow-band bandpass filters and it has been suggested by Temes (8) that they may yield robust bandpass $\Sigma\Delta$ modulators.

4. COMPONENT SPECIFICATIONS

4.1 Capacitor ratios

Capacitor ratios were chosen to correctly set the NTF and STF of the cascade-of-resonators structure of Figure 5, and were then adjusted to scale the circuit for maximum dynamic range. As the bandpass $\Sigma\Delta$ concept is new, and the effects of clipping are not yet understood, a conservative L_1 -norm was used. Integrator output swings were found for a variety of small inputs, and scaling was based on the worst-case values, plus a 10% safety margin.

The scaled capacitor ratios are given in Figure 7 together with a single-ended representation of the modulator. In this single-ended circuit (with positive capacitors) the A coefficients can only be positive as they are implemented with non-inverting feed-ins, whereas the B and R coefficients can only be negative as they are implemented with inverting feed-ins. These restrictions result in the need for a differential design, which realises negative capacitor ratios by making polarity-reversed connections to the differential op-amp outputs. Clock phasing was chosen for compatibility with an existing design.

4.2 Absolute Capacitor Sizes

Minimum capacitor sizes are determined by noise constraints. The kT/C noise present on each switched capacitor is assumed to have a white spectrum, and is spread from 0 to π . As we are concerned strictly with in-band noise, we gain an oversampling-factor reduction in this kT/C noise power. This allows the minimum allowable capacitor size to be reduced by the same factor, and proves to be an added benefit of oversampling. Additionally, certain capacitors see noise-shaped transfer functions to the output, again reducing noise power at the output and hence minimum capacitor size. The result of these considerations is that the capacitors with the largest contributions to circuit noise are in the first resonator: C_{i0} , C_{i1} , C_{x1} and C_{r1} .

Maximum capacitor sizes are determined by bandwidth and slew-rate constraints. Given specific op-amp performance, capacitors must be small enough to allow sufficient amplifier settling.

4.3 Op-Amp DC Gain

Operational amplifiers with high DC gain are necessary to maintain the desired transfer functions. Each resonator in our structure includes two op amps and is responsible for a complex conjugate pair of zeros of H . Finite op-amp gain in a resonator shifts both the radius and the angle of these zeros, thereby reducing in-band attenuation and increasing N_0^2 . The poles of H also shift, but their affect on N_0^2 is minimal. For the modulator and structure under

consideration, finite 60 dB op-amp gain increases N_0^2 by a negligible 0.6 dB, whereas 50 dB opamp gain increases N_0^2 by a more significant 3.8 dB

4.4 Op-Amp Speed

Satisfactory op-amp bandwidth and slew-rate performance are necessary to ensure that sufficient settling occurs. For a given capacitive load, fast settling requires large transistors and large bias currents.

As is the case with lowpass $\Sigma\Delta$ convertors, it is possible that integrator outputs will change by their maximum swing in each clock cycle. Thus, bandpass $\Sigma\Delta$ convertors have settling requirements that are no more stringent than those of lowpass $\Sigma\Delta$ convertors.

4.5 Simulation Results

The linear model predicts an SNR of 78 dB for a half-scale input when tuned to the low end of the AM band. Under identical conditions, a *time-domain* simulation of the ideal modulator shows that the SNR is actually 84 dB. This discrepancy is due to the inaccuracy of the assumption that the powerspectral density of the quantisation noise is $1/3$ at all frequencies

A simulation of the circuit shown in Figure 7 was performed using the SWITCAP2 simulation program (Suyama et al (9)). Figure 8 plots the *spectrum of the* output bit-stream which clearly *shows the* band-reject noise-shaping. Analysis on the bit-stream found an SNR of 84 dB for the half-scale tone input which agrees with the previous time-domain simulation.

5. DECIMATION AND DEMODULATION

As introduced in Schreier and Snelgrove (10), a complex modulator and (multiplexed) complex lowpass filter can be used to achieve reduction in the bit rate to a manageable level. In this scheme, the bit-stream is modulated down to baseband by multiplying it by $e^{-j\omega_0 t}$. The resulting real and imaginary streams are then lowpass-filtered using conventional means.

A band location of $\omega_0 = \pi/2$ makes this process particularly easy, as the multiplying signal is simply

$$e^{-j\omega_0 t} = (1, 0, -1, 0, \dots) + j(0, -1, 0, 1, \dots), \quad (3)$$

so that the product is a pair of interleaved bit-streams, each with half the bit-rate of the original stream. These streams must be lowpass-filtered and downsampled, and (11) provides a simple scheme for an initial stage of decimation.

Further decimation is needed to reduce the bit rate to the Nyquist rate. To maintain 14-bit accuracy, filtering must adequately reject the out-of-band noise that will fold into the band of interest. A DSP can be configured for this stage, and must be able to accept a variable-rate input and must have adjustable lowpass filter bandwidth.

By using a DSP to do the last stage of decimation and demodulation, one gains considerable flexibility since software can be used to handle the multitude of standards present in AM stereo.

6. CONCLUSIONS

An AM receiver using an analogue-to-digital convertor based on a bandpass $\Sigma\Delta$ modulator was designed. Simulations predict 14-bit performance even in the face of circuit non-idealities. A solution to the decimation problem is known and consequently no barriers to the success of this circuit are anticipated.

REFERENCES

1. Candy, J.C., and Temes, G.C., 1991, "Oversampling Methods for A/D and D/A Conversion" in Oversampling Delta-Sigma Converters, eds. J.C. Candy and G.C. Temes, IEEE Press, in press.
2. Norsworthy, S., Post, I.G., and Fetterman, H.S., 1989, "A 14-bit 80-kHz Sigma-Delta A/D Converter: Modeling, Design, and Performance Evaluation," *IEEE Journal of Solid-State Circuits*, 24, 256-266.
3. Boser, B.E., and Wooley, B.A., 1988, "The Design of Sigma-Delta Modulation Analog-to-Digital Converters," *IEEE Journal of Solid-State Circuits*, 23, 1298-1308.
4. Schreier, R., and Snelgrove, M., 1989, "Bandpass Sigma-Delta Modulation," *Electronics Letters*, 25, 1560-1561.
5. Lee, W.L., 1987, "A Novel Higher Order Interpolative Modulator Topology for High Resolution A/D Converters," Massachusetts Institute of Technology, S. M. Thesis.
6. Ferguson, P.F.Jr., Ganesan, A., and Adams, R.W., 1990, "One Bit Higher Order Sigma-Delta A/D Converters," *Proc. IEEE Int. Symp. on Circuits and Systems*, 890-893.
7. Gregorian, R., and Temes, G.C., 1986, "Analog MOS Integrated Circuits for Signal Processing", Wiley, New York, 363-387.
8. Temes, G.C., 1991, private communication.
9. Suyama, K., Fang, S-C., and Tsvividis, Y.P., 1990, "Simulation of Mixed Switched-Capacitor/Digital Networks with Signal-Driven Switches," *IEEE Journal of Solid-State Circuits*, 25, 1403-1413.
10. Schreier, R., and Snelgrove, M., 1990, "Decimation for Bandpass Sigma-Delta Analog-to-Digital Conversion," *Proc. IEEE Int. Symp. on Circuits and Systems*, 1801-1804.
11. Candy, J.C., 1986, "Decimation for Sigma Delta Modulation," *IEEE Transactions on Communications*, 34, 72-76.

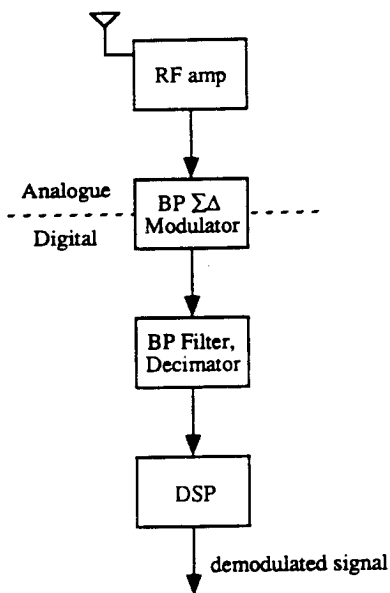


Figure 1 The block diagram of the proposed digital AM radio.

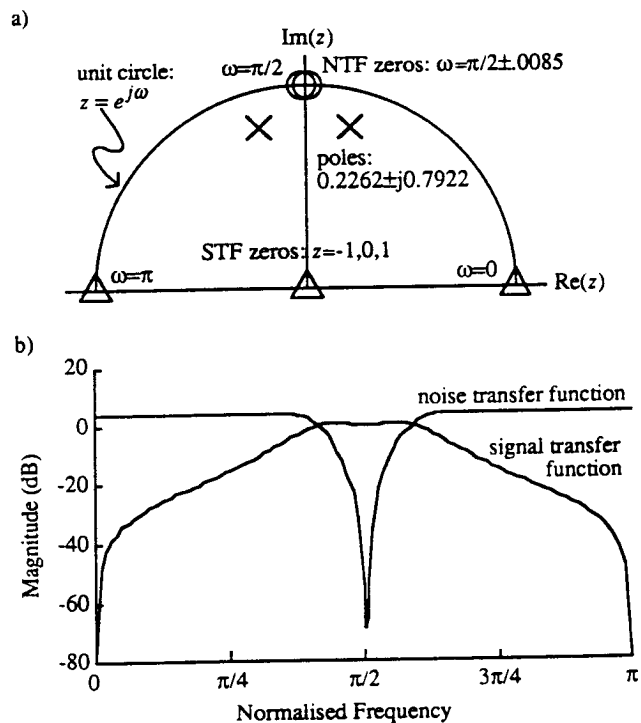


Figure 2 The noise and signal transfer functions for the optimised-zero fourth-order modulator. a) Pole/zero locations in the upper-half of the z -plane. b) Magnitude response.

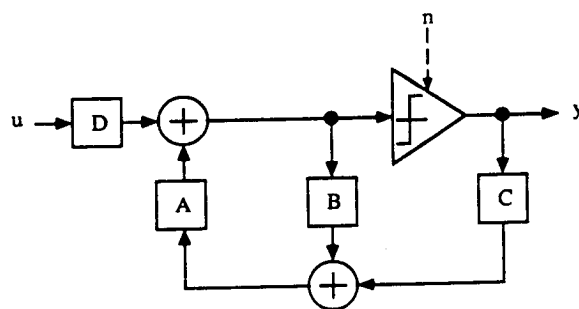


Figure 3 A general topology for a single-quantiser sigma-delta modulator.

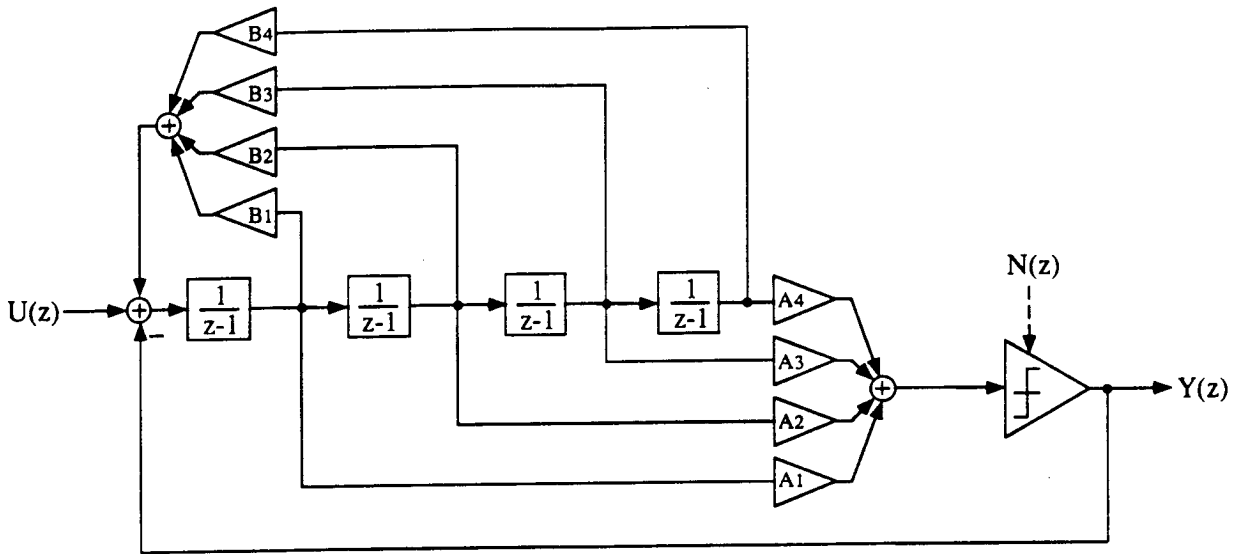


Figure 4 The cascade-of-integrators structure.

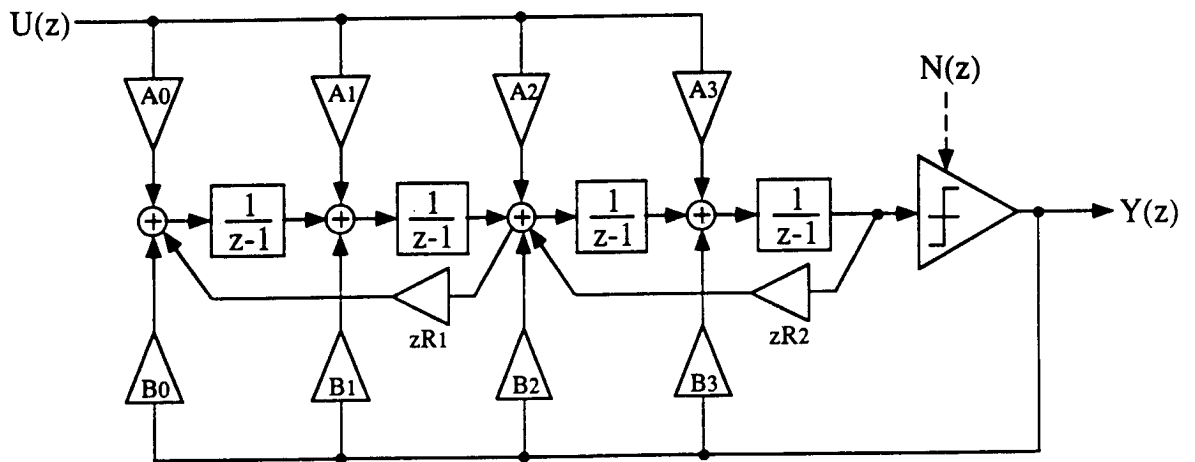


Figure 5 The cascade-of-resonators structure.

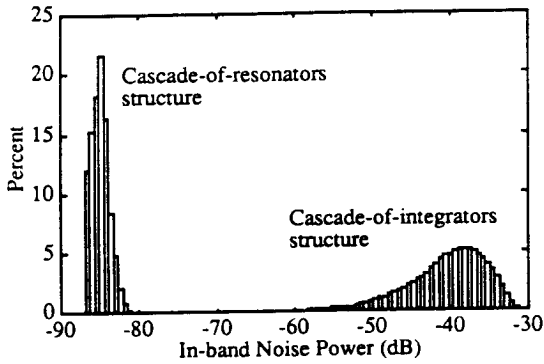


Figure 6 Modulator performance under the influence of random capacitor-ratio errors for two modulator structures.

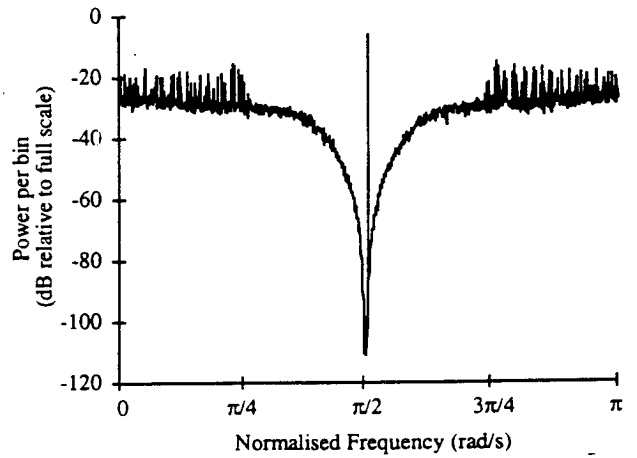
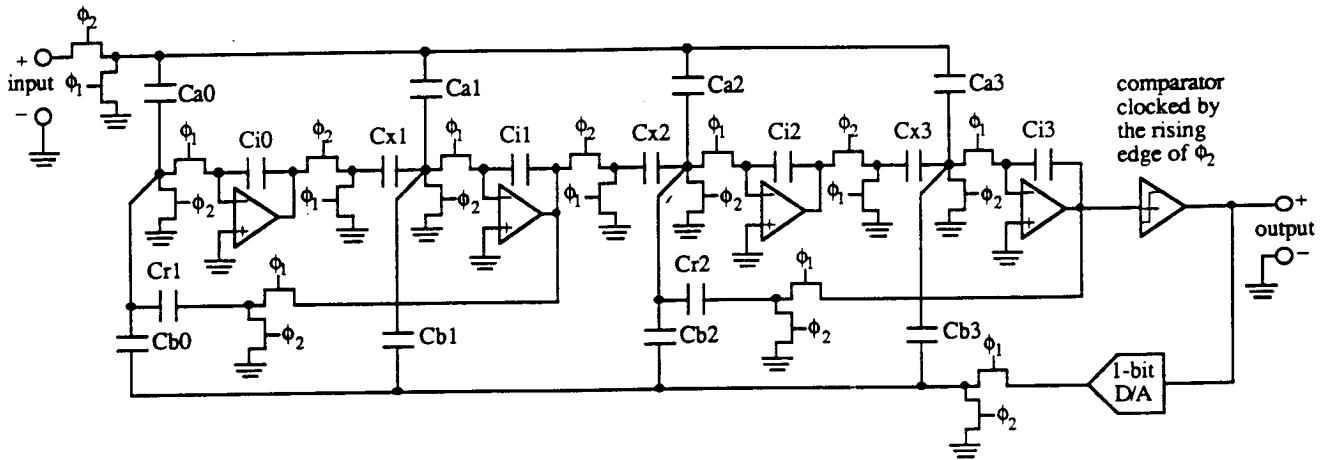


Figure 8 Spectrum of the modulator output for a half-scale tone input near the upper edge of the band of interest. The abscissa contains 1024 bins.



parameter	R_1	A_0	B_0	X_1	A_1	B_1	X_2	R_2	A_2	B_2	X_3	A_3	B_3
initial coefficient	-1.9832	-0.3093	-0.2926	1.	-0.3068	0.0142	1.	-2.0168	0.156	0.8457	1.	0.1534	0.
scaled coefficient	-1.3457	-0.221	-0.209	1.4737	-0.3229	0.015	0.38	-1.2908	0.0624	0.3383	1.5625	0.0959	0.
capacitor ratio	1.3457	-0.221	0.209	1.4737	-0.3229	-0.015	0.38	1.2908	0.0624	-0.3383	1.5625	0.0959	0.

Figure 7 A single-ended representation of a fourth-order modulator with the cascade-of-resonators structure.